

WASP-25b: a $0.6 M_J$ planet in the Southern hemisphere.

B. Enoch¹*, A. Collier Cameron¹, D.R. Anderson², T.A. Lister³, C. Hellier², P.F.L. Maxted², D. Queloz⁴, B. Smalley², A.H.M.J. Triaud⁴, R.G. West⁵, D.J.A. Brown¹, M. Gillon^{6,4}, L. Hebb⁷, N. Parley¹, F. Pepe⁴, D. Pollacco⁸, D. Segransan⁴, E. Simpson⁸, R.A. Street³ and S. Udry⁴

¹School of Physics and Astronomy, University of St. Andrews, North Haugh, St Andrews, KY16 9SS.

²Astrophysics Group, Keele University, Staffordshire, ST5 5BG, UK.

³Las Cumbres Observatory, 6740 Cortona Drive Suite 102, Goleta, CA 93117, USA.

⁴Observatoire astronomique de l'Université de Genève, 51 Chemin des Maillettes, 1290 Sauverny, Switzerland.

⁵Department of Physics and Astronomy, University of Leicester, Leicester, LE1 7RH, UK.

⁶Institut d'Astrophysique et de Géophysique, Université de Liège, Allée de 6 Août, 17, Bat B5C, Liège 1, Belgium.

⁷Vanderbilt University, Department of Physics and Astronomy, Nashville, TN 37235.

⁸Astrophysics Research Centre, School of Mathematics & Physics, Queen's University, University Road, Belfast, BT7 1NN, UK.

Received / Accepted

ABSTRACT

We report the detection of a $0.6 M_J$ extrasolar planet by WASP-South, WASP-25b, transiting its solar-type host star every 3.76 days. A simultaneous analysis of the WASP and FTS photometry and CORALIE spectroscopy yields a planet of $R_p = 1.26 R_J$ and $M_p = 0.58 M_J$ around a slightly metal-poor solar-type host star, $[Fe/H] = -0.05 \pm 0.10$, of $R_* = 0.95 R_\odot$ and $M_* = 1.00 M_\odot$. WASP-25b is found to have a density of $\rho_p = 0.29 \rho_J$, a low value for a sub-Jupiter mass planet. We investigate the relationship of planetary radius to planetary equilibrium temperature and host star metallicity for transiting exoplanets with a similar mass to WASP-25b. We find that the relation $R_p = 0.3691 - 0.3481[Fe/H] + 6.309(T_{eq}/1000)$ matches the observed radii of these planets.

Key words: planetary systems

1 INTRODUCTION

To date, over 440 exoplanets have been discovered, including more than 70 detected by the transit method¹. The transit method together with follow-up radial velocity observations allow measurement of both the mass and radius of the planet, leading to a value for the planet's bulk density (Charbonneau et al. 2000). The atmospheric composition of transiting exoplanets can also be investigated through high-precision photometric and spectroscopic measurements, see e.g. Charbonneau et al. (2002).

A wide range of transiting exoplanets radii has been found and there has been much investigation into the factors that may influence a planet's radius. For example, Guillot et al. (2006) propose a negative relationship between the metallicity of a host star and the radius of an orbiting planet, caused by an increase in the amount of heavy elements in the planet, leading to a more massive core and hence smaller radius for a given mass. Alternatively, Burrows et al. (2007) consider that increasing the metallicity may increase

the opacity of an exoplanet's atmosphere, retarding cooling and leading to a larger radius for a given mass. Another influence on a planet's radius may be the equilibrium temperature of the planet (Guillot & Showman 2002), determined by the stellar irradiation and the planet's distance from its host star. Tidal heating due to the circularisation of the orbits of close-in exoplanets may also play a role in inflating the planetary radius (Bodenheimer et al. 2003; Jackson et al. 2008). One motivation of the SuperWASP project is to detect enough transiting exoplanets, with a wide range of orbital and compositional parameters, to allow analyses that may distinguish between such differing models.

In this paper, we report the discovery of a $0.6 M_J$ planet orbiting a solar-mass star, WASP-25 (=TYC6706-861-1, =1SWASP J130126.36-273120.0), in the southern hemisphere. Analysis of photometric and spectroscopic data reveals WASP-25b to be another low-density planet, comparable to HD 209458b (Charbonneau et al. 2000). We also analyse the dependence of the radii of planet's of similar mass to WASP-25b, including 7 other WASP planets, on host star metallicity and planetary equilibrium temperature, finding an excellent agreement between observed and calibrated radii.

* E-mail: becky.enoch@st-andrews.ac.uk

¹ www.exoplanet.eu

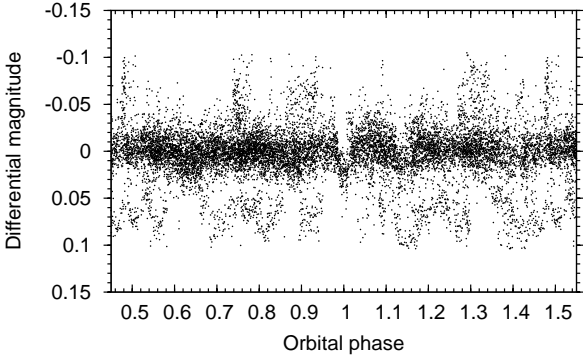


Figure 1. WASP discovery lightcurve folded on the orbital period of $P = 3.765$ d. Points with error above $3 \times \text{median}$ were clipped, where $\text{median} = 0.012$ mag

In Section 2 we describe the photometric and spectroscopic observations and data reduction procedures. In Section 3 we present the stellar and planetary parameters extracted from these data. Finally, in Section 4 we compare WASP-25b with the ensemble of known planets of similar mass, and examine the relationship between stellar metallicity, irradiating flux and planet radius.

2 OBSERVATIONS

2.1 Photometric Observations

The WASP-South observatory is located at SAAO in South Africa, and consists of eight 11cm telescopes of $7.8^\circ \times 7.8^\circ$ field of view each, on a single fork mount. The cameras scan repeatedly through eight to ten sets of fields, taking 30 second exposures. See Pollacco et al. (2006) for more details on the WASP project and the data reduction procedure, and Collier Cameron et al. (2007) and Pollacco et al. (2008) for an explanation of the candidate selection process.

WASP-25 was observed by WASP-South in 2006, 2007 and 2008, producing a total of 14,186 photometric datapoints. The 2007 dataset showed the transit event most clearly, detected at a period of 3.76 days. Figure 1 shows the WASP-South discovery lightcurve, using data from all seasons.

Further photometric observations were subsequently obtained on 2010 April 3 using the LCOGT 2m Faulkes Telescope South (FTS) at Siding Spring, Australia. Observations were obtained using the fs01 Spectral camera containing a 4096×4096 pixel Fairchild CCD which was binned 2×2 giving 0.303 arcsec/pixel and a field of view of $\sim 10' \times 10'$. 285 datapoints were obtained through a Pan-STARRS z filter, capturing an entire transit.

The data were pre-processed through the WASP Pipeline (Pollacco et al. 2006) to perform masterbias/flat creation, debiassing and flatfield correction in the standard manner. Object detection and aperture photometry was performed using the DAOPHOT (Stetson 1987) package within the IRAF environment² with an aperture size of 18 binned pixels. Differential magnitudes of WASP-25 were formed by a weighted combination of the flux relative to 26 comparison stars within the field of view

² IRAF is distributed by the National Optical Astronomy Observatory, which is operated by the Association of Universities for Research in Astronomy (AURA) under cooperative agreement with the National Science Foundation.

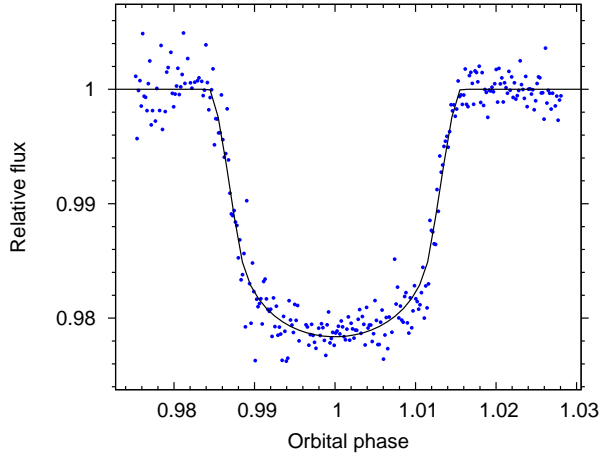


Figure 2. FTS follow-up photometry of WASP-25 on 3 April 2010. The central transit time is at HJD = 5290.05617.

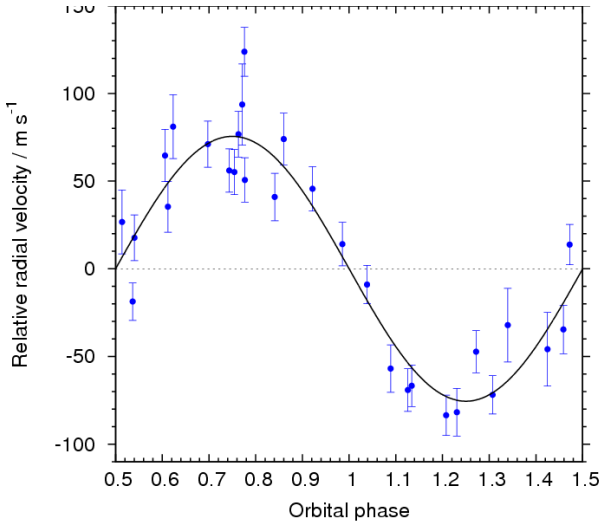


Figure 3. Top plot: Radial velocity measurements. The solid line is the best-fitting MCMC solution. The centre-of-mass velocity, $\gamma = -2.63236$ km s^{-1} , was subtracted. Bottom plot: Bisector spans (BS), with $\sigma_{\text{BS}} = 2\sigma_{\text{RV}}$.

2.2 Spectroscopic Observations

WASP-25, a $V_{\text{mag}} = 11.9$ star, was observed 29 times with the CORALIE spectrograph on the 1.2m Euler telescope, between 29 December 2008 and 28 June 2009. The spectra were processed using the standard data reduction pipeline for CORALIE (Baranne et al. 1996; Mayor et al. 2009), plus a correction for the blaze function (Triaud & et al 2010). These data are given in Table 1 and shown phase-folded in Figure 3: the low-amplitude radial velocity variations and the lack of correlation between the bisector spans and radial velocity, shown in Figure 4, are consistent with a planet-mass object orbiting the host star.

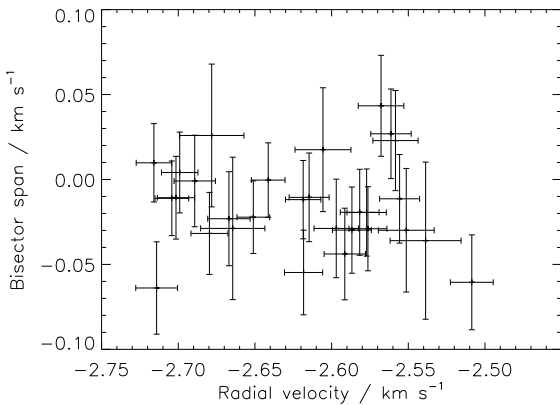
3 SYSTEM PARAMETERS

3.1 Stellar Parameters

The CORALIE spectra were placed on a common wavelength scale and co-added to produce a higher signal-to-noise spectrum, allow-

Table 1. CORALIE radial velocity measurements of WASP-25

BJD–2 400 000	RV (km s $^{-1}$)	σ_{RV} (km s $^{-1}$)	BS (km s $^{-1}$)
54829.8227	-2.577	0.013	-0.019
54896.7698	-2.651	0.011	-0.022
54940.7092	-2.716	0.012	0.010
54941.7043	-2.619	0.012	-0.012
54942.7257	-2.576	0.012	-0.029
54943.6374	-2.618	0.012	-0.055
54944.7155	-2.680	0.012	-0.032
54945.7265	-2.615	0.013	-0.011
54946.6166	-2.582	0.013	-0.019
54947.6016	-2.641	0.011	-0.000
54947.7912	-2.689	0.013	0.001
54948.6130	-2.704	0.011	-0.011
54949.8031	-2.551	0.018	-0.030
54950.6221	-2.591	0.013	-0.044
54951.6953	-2.701	0.012	-0.011
54971.6453	-2.678	0.021	0.026
54972.6724	-2.561	0.013	0.027
54973.5157	-2.587	0.013	-0.030
54974.6787	-2.714	0.014	-0.064
54975.5379	-2.667	0.014	-0.023
54976.6837	-2.556	0.013	-0.011
54982.6194	-2.664	0.021	-0.029
54983.6213	-2.568	0.015	0.043
54983.6446	-2.597	0.015	-0.029
54984.5785	-2.558	0.015	0.023
54985.6100	-2.699	0.012	0.004
54995.5555	-2.509	0.014	-0.061
55009.6287	-2.606	0.018	0.018
55010.5967	-2.539	0.023	-0.036

**Figure 4.** Bisector spans versus radial velocity, where bisector uncertainties are taken to be equal to twice the radial velocity uncertainties.

ing an analysis of the host star and thus measurement of the stellar temperature, gravity, metallicity, $v \sin i$ and elemental abundances, given in Table 2, where η is microturbulence. The spectral data were analysed using the UCLSYN spectral synthesis package (Smalley et al. 2001) and ATLAS9 models without convective overshooting (Castelli et al. 1997). The effective temperature and $\log g$ were determined using the H α and H β lines, and the Na I D and Mg I b lines respectively, while the Ca H and K lines provided a check on those values. Further details of the spectral analysis are given in West et al. (2009). The analysis yielded $T_{\text{eff}} = 5750 \pm 100$ K and $[\text{Fe}/\text{H}] = -0.05 \pm 0.10$.

[!h]

Table 2. Stellar Parameters of WASP-25

Parameter	Value
T_{eff}	5750 ± 100 K
$\log g$	4.5 ± 0.15
η	1.1 ± 0.1 km s $^{-1}$
$v \sin i$	3.0 ± 1.0 km s $^{-1}$
Spectral Type	G4
[Fe/H]	-0.05 ± 0.10
[Si/H]	0.00 ± 0.06
[Ca/H]	0.08 ± 0.14
[Ti/H]	0.04 ± 0.07
[Ni/H]	-0.08 ± 0.10
$\log[\text{Li}/\text{H}]$	1.63 ± 0.09
V (mag)	11.88
1 SWASP J130126.36-273120.0	

3.2 System Parameters

The WASP-South and FTS photometry were simultaneously analysed with the CORALIE radial velocity data in a Markov-Chain Monte-Carlo (MCMC) analysis. This analysis is described in Collier Cameron et al. (2007), but is here modified as described in Enoch et al. (2010) to determine stellar mass and radius using a calibration on T_{eff} , $\log \rho$ and $[\text{Fe}/\text{H}]$ (similar to the T_{eff} , $\log g$ and $[\text{Fe}/\text{H}]$ calibration described in Torres et al. (2009)). The temperature and metallicity were obtained through spectral analysis (given in Table 2), and the density is determined directly from the photometry. Mass and radius values obtained for other WASP host stars via this method agree closely with values obtained through isochrone analysis.

An initial analysis was performed allowing the eccentricity value to float, producing a value of $e = 0.114^{+0.047}_{-0.044}$. This eccentricity value is consistent with 0 at the 3σ level, and was suspected to not be significant, as can occur from spurious asymmetries in quadrature fits due to noise (Laughlin et al. 2005), so a second analysis was performed with eccentricity fixed to 0. We performed an F-test on the radial velocity residuals from the circular and floating eccentricity fits, resulting in a value of 0.897 which shows that the eccentric fit is not significant.

The resulting circular model best-fit parameters for the star–planet system are listed in Table 3, using the best-fit parameters from the $e = 0$ fit and the uncertainties from the fit allowing eccentricity to float, to sufficiently account for uncertainty due to unknown eccentricity. The results show WASP-25 to be a solar analogue of one solar mass and 0.95 ± 0.04 solar radius, and WASP-25b to be a bloated hot Jupiter of $0.58 \pm 0.04 M_J$ and $1.26 \pm 0.06 R_J$, giving a planet density of $\rho = 0.29^{+0.04}_{-0.03} \rho_J$.

The stellar density of $1.18^{+0.12}_{-0.11} \rho_\odot$ obtained from the MCMC analysis was used along with the determined stellar temperature and metallicity values in an interpolation of the Girardi et al. (2000) stellar evolution tracks, see Figure 5. Using the best-fit metallicity of -0.06 indicates that WASP-25 has a mass of $0.99 \pm 0.04 M_\odot$, agreeing well with the calibrated MCMC result, and an age of 2.5 ± 2.1 Gyr.

Table 3. System Parameters of WASP-25

Parameter	Symbol	Value
Period (days)	P	3.76483 ± 0.00005
Transit Epoch (HJD)	T_0	5259.93733 ± 0.00023
Transit duration (days)	D	0.117 ± 0.001
Planet/Star area ratio	R_p^2/R_*^2	0.0188 ± 0.0003
Impact Parameter	b	$0.43^{+0.07}_{-0.09}$
Stellar Reflex Velocity (ms^{-1})	K_1	75.5 ± 5.1
Centre-of-mass Velocity (ms^{-1})	γ	-2632.4 ± 0.6
Orbital separation (AU)	a	0.0474 ± 0.0004
Orbital inclination (deg)	i	87.7 ± 0.5
Orbital eccentricity	e	0.0
Stellar mass (M_\odot)	M_*	1.00 ± 0.03
Stellar radius (R_\odot)	R_*	0.95 ± 0.04
Stellar surface gravity ($\log g_*$)	$\log g_*$	4.49 ± 0.03
Stellar density (ρ_\odot)	ρ_*	$1.18^{+0.12}_{-0.10}$
Stellar metallicity	[Fe/H]	-0.06 ± 0.10
Stellar effective temperature	T_{eff}	5712 ± 100
Planet mass (M_J)	M_p	0.58 ± 0.04
Planet radius (R_J)	R_p	1.26 ± 0.06
Planet surface gravity ($\log g_J$)	$\log g_p$	2.92 ± 0.04
Planet density (ρ_J)	ρ_p	$0.288^{+0.037}_{-0.029}$
Planet temperature (A=0, F=1) (K)	T_{eq}	1231 ± 40

4 DISCUSSION

A density of $0.29^{+0.04}_{-0.03} \rho_J$ places WASP-25b amongst the bloated hot Jupiters, with over 80% of known transiting exoplanets being more dense³. Guillot et al. (2006) proposed a correlation between the metallicity of a host star and the amount of heavy elements present in the planet. A larger amount of heavy elements is likely to produce a more massive rocky core and hence would lead to larger planetary radii for lower metallicity stars, for a given planetary mass (Fressin et al. 2007). Alternatively, the heavy elements could increase the opacity of the planetary interior, potentially increasing the radius (Burrows et al. 2007). We plot the radii against host star metallicity of 19 planets of a similar mass to WASP-25b ($0.4\text{--}0.7 M_J$ - see Table 4 for details) in Figure 6, shown with a least absolute deviation linear fit overplotted. WASP-25b is plotted with a diamond around the cross. The two significant outliers at $[\text{Fe}/\text{H}] = 0.45$ and 0.34 are XO-2b (Burke et al. 2007) and Kepler-6b (Dunham et al. 2010) respectively.

The correlation coefficient of these radii and metallicities is -0.51 , showing a moderate negative relationship. The negative slope implies that the effect of a massive core outweighs the effect of increased opacity in the interior of the planet. Metal-rich stars

thus tend to spawn planets with bigger cores, giving them slightly smaller radii at a given mass.

For a given planet mass, an alternative influence on the radius of an exoplanet is the planet's equilibrium temperature (Fressin et al. 2007), T_{eq} , defined as

$$T_{\text{eq}} = T_{\ast,\text{eff}} \sqrt{\frac{R_*}{2a}} \quad (1)$$

where $T_{\ast,\text{eff}}$ is the host star's effective temperature, R_* is the stellar radius and a is the semi-major axis. We find the correlation between the equilibrium temperature and radius of these 20 planets to be 0.70, a strong relationship, shown in Figure 7.

Since both the host star metallicity and the planet's equilibrium temperature explain the planetary radii in part, we performed a weighted Singular Value Decomposition (SVD) fit to fully quantify the relationship. This resulted in the equation

$$\rho_p = 0.3691 - 0.3481[\text{Fe}/\text{H}] + 6.309(T_{\text{eq}}/1000K) \quad (2)$$

producing a very good fit to the planetary radii, as shown in Figure 8.

Many of the planets considered here have orbital eccentricities too small to measure reliably with the data currently available. Nonetheless, the strength of the radius-metallicity-irradiation correlation appears to account for most of the variation in planet

² www.exoplanet.eu

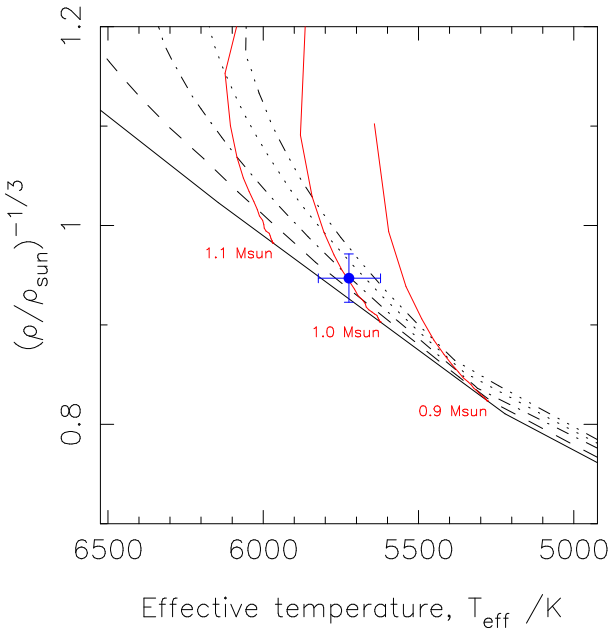


Figure 5. Isochrone tracks from Girardi et al. (2000) for WASP-25 using the best-fit metallicity of -0.06 .

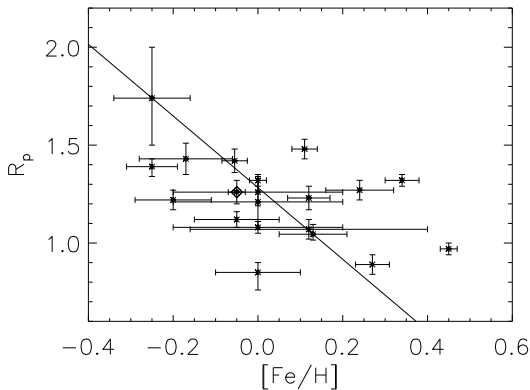


Figure 6. Radius versus metallicity of planets of $0.4–0.7 M_J$.

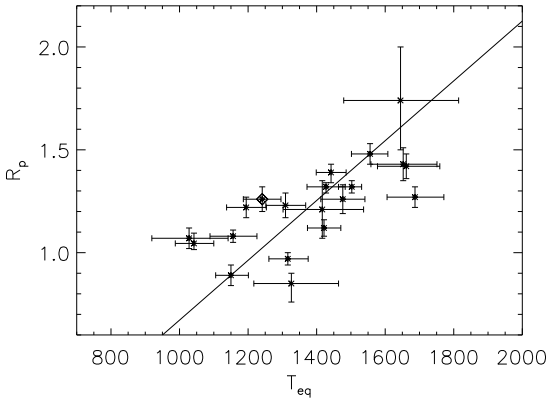


Figure 7. Radius versus equilibrium temperature of planets of $0.4–0.7 M_J$.

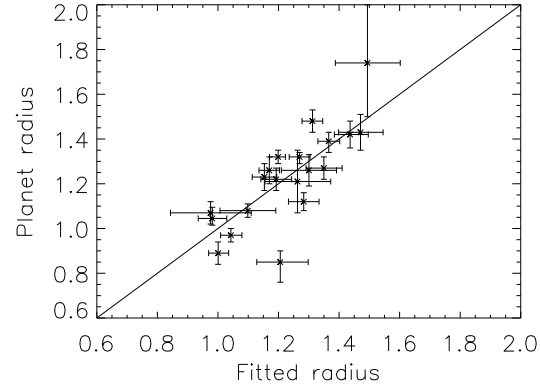


Figure 8. Results of SVD fit on the radii of planets of $0.4–0.7 M_J$.

radii in this mass range, suggesting that past or present tidal heating plays a relatively minor role in supporting inflated planets.

5 CONCLUSIONS

We have reported the detection of a $0.58 M_J$ planet, WASP-25b, transiting a slightly metal-poor solar-mass star in the southern hemisphere with an orbital period of 3.76 days. WASP-25b has a low density, $0.29 \rho_J$, and we investigate its bloated radius, $R_p = 1.26 R_J$. We find that the radii of transiting exoplanets of a similar mass to WASP-25b can be explained well by a calibration to the host star metallicity and planetary equilibrium temperature.

ACKNOWLEDGEMENTS

WASP-South is hosted by the South African Astronomical Observatory and we are grateful for their ongoing support and assistance. Funding the WASP comes from consortium universities and from the UK’s Science and Technology Facilities Council.

REFERENCES

- Alonso R., Brown T. M., Torres G., Latham D. W., Sozzetti A., Mandushev G., Belmonte J. A., Charbonneau D., Deeg H. J., Dunham E. W., O’Donovan F. T., Stefanik R. P., 2004, ApJL, 613, L153
- Anderson D. R., Hellier C., Gillon M., Triaud A. H. M. J., Smalley B., Hebb L., Collier Cameron A., Maxted P. F. L., Queloz D., West R. G., Bentley S. J., Enoch B., Horne K., Lister T. A., Mayor M., Parley N. R., et al 2010, ApJ, 709, 159
- Bakos J. Á., Noyes R. W., Kovács G., Latham D. W., Sasselov D. D., Torres G., Fischer D. A., Stefanik R. P., Sato B., Johnson J. A., Pál A., Marcy G. W., Butler R. P., Esquerdo G. A., et al 2007, ApJ, 656, 552
- Baranne A., Queloz D., Mayor M., Adrianzyk G., Knispel G., Kohler D., Lacroix D., Meunier J., Rimbaud G., Vin A., 1996, A&Asupp, 119, 373
- Bodenheimer P., Laughlin G., Lin D. N. C., 2003, ApJ, 592, 555
- Burke C. J., McCullough P. R., Valenti J. A., Summers F. J., Stys J. E., Johns-Krull C. M., Janes K. A., Heasley J. N., Bissinger R., Fleenor M., Foote C. N., Garcia-Melendo E., Gary B. L., Howell

Table 4. Details of the 12 planets of a similar mass to WASP-25b.

Planet	M_p	R_p	a	T_{eff}	[Fe/H]	R_*	T_{eq}	Reference
Kepler-7	0.43	$1.48^{+0.05}_{-0.05}$	$0.0622^{+0.0011}_{-0.0008}$	5933 ± 44	0.11 ± 0.03	$1.84^{+0.07}_{-0.07}$	1556^{+52}_{-54}	Latham et al. (2010)
WASP-11	0.46	$1.045^{+0.05}_{-0.03}$	$0.043^{+0.002}_{-0.002}$	4980 ± 60	0.13 ± 0.08	$0.81^{+0.03}_{-0.03}$	1042^{+58}_{-55}	West et al. (2009)
WASP-13	0.46	$1.21^{+0.14}_{-0.14}$	$0.0527^{+0.0017}_{-0.0019}$	5826 ± 100	0.0 ± 0.2	$1.34^{+0.13}_{-0.13}$	1416^{+121}_{-114}	Skillen et al. (2009)
CoRoT-5	0.47	$1.39^{+0.04}_{-0.05}$	$0.0495^{+0.0003}_{-0.0003}$	6100 ± 65	-0.25 ± 0.06	$1.19^{+0.04}_{-0.04}$	1442^{+44}_{-43}	Rauer et al. (2009)
WASP-17	0.49	$1.74^{+0.26}_{-0.24}$	$0.0501^{+0.0017}_{-0.0018}$	6500 ± 100	-0.25 ± 0.09	$1.38^{+0.19}_{-0.19}$	1645^{+169}_{-166}	Anderson et al. (2010)
WASP-6b	0.50	$1.22^{+0.05}_{-0.05}$	$0.0421^{+0.0008}_{-0.0013}$	5450 ± 100	-0.20 ± 0.09	$0.87^{+0.03}_{-0.04}$	1195^{+59}_{-57}	Gillon et al. (2009)
HAT-1b	0.52	$1.23^{+0.06}_{-0.06}$	$0.0553^{+0.0014}_{-0.0014}$	6047 ± 56	0.12 ± 0.05	$1.12^{+0.05}_{-0.05}$	1309^{+59}_{-57}	Bakos et al. (2007)
OGLE-111b	0.53	$1.07^{+0.05}_{-0.05}$	$0.047^{+0.001}_{-0.001}$	5070 ± 400	0.12 ± 0.28	$0.83^{+0.03}_{-0.03}$	1028^{+114}_{-109}	Pont et al. (2004)
WASP-15b	0.54	$1.43^{+0.08}_{-0.08}$	$0.0499^{+0.0018}_{-0.0018}$	6300 ± 100	-0.17 ± 0.11	$1.48^{+0.07}_{-0.07}$	1653^{+99}_{-94}	West et al. (2009)
WASP-22	0.56	$1.12^{+0.04}_{-0.04}$	$0.0468^{+0.0004}_{-0.0004}$	6000 ± 100	-0.05 ± 0.1	$1.13^{+0.03}_{-0.03}$	1421^{+49}_{-48}	Maxted et al. (2010)
XO-2b	0.57	$0.97^{+0.03}_{-0.03}$	$0.037^{+0.002}_{-0.002}$	5340 ± 32	0.45 ± 0.02	$0.96^{+0.02}_{-0.02}$	1315^{+59}_{-55}	McCullough et al. (2006)
WASP-25b	0.58	$1.26^{+0.06}_{-0.06}$	$0.0474^{+0.0004}_{-0.0004}$	5750 ± 100	-0.05 ± 0.02	$0.95^{+0.04}_{-0.04}$	1241^{+55}_{-55}	-
HAT-3b	0.60	$0.89^{+0.05}_{-0.05}$	$0.0389^{+0.0007}_{-0.0007}$	5185 ± 46	0.27 ± 0.04	$0.82^{+0.04}_{-0.04}$	1150^{+51}_{-45}	Torres et al. (2007)
Kepler-8b	0.60	$1.42^{+0.06}_{-0.06}$	$0.0483^{+0.0006}_{-0.0012}$	6213 ± 150	-0.055 ± 0.03	$1.49^{+0.06}_{-0.06}$	1662^{+98}_{-84}	Jenkins et al. (2010)
TrES-1b	0.61	$1.08^{+0.03}_{-0.03}$	$0.0393^{+0.0007}_{-0.0007}$	5250 ± 200	0.0 ± 0.2	$0.82^{+0.02}_{-0.02}$	1156^{+70}_{-67}	Alonso et al. (2004)
OGLE-10b	0.63	$1.26^{+0.07}_{-0.07}$	$0.04162^{+0.0004}_{-0.0004}$	5800 ± 100	0.0 ± 0.2	$1.16^{+0.06}_{-0.06}$	1476^{+65}_{-64}	Konacki et al. (2005)
Kepler-6b	0.67	$1.32^{+0.03}_{-0.03}$	$0.0457^{+0.0006}_{-0.0005}$	5647 ± 44	0.34 ± 0.04	$1.39^{+0.02}_{-0.03}$	1503^{+29}_{-39}	Dunham et al. (2010)
WASP-7	0.67	$0.85^{+0.05}_{-0.09}$	$0.0618^{+0.0014}_{-0.0033}$	6166 ± 250	0.0 ± 0.1	$1.23^{+0.08}_{-0.08}$	1326^{+138}_{-110}	Hellier et al. (2009)
HAT-4b	0.68	$1.27^{+0.05}_{-0.05}$	$0.0446^{+0.0012}_{-0.0012}$	5860 ± 80	0.24 ± 0.08	$1.59^{+0.07}_{-0.07}$	1687^{+84}_{-82}	Kovács et al. (2007)
HD 209458b	0.69	$1.32^{+0.02}_{-0.03}$	$0.0471^{+0.0005}_{-0.0005}$	6000 ± 50	0.0 ± 0.2	$1.15^{+0.06}_{-0.06}$	1427^{+56}_{-56}	Charbonneau et al. (2000)

P. J., Mallia F., Masi G., Vanmunster T., 2007, in Bulletin of the American Astronomical Society Vol. 38 of Bulletin of the American Astronomical Society, XO-2b: A Transiting Hot Jupiter in a Metal-rich Common Proper Motion Binary. pp 145–+

Burrows A., Hubeny I., Budaj J., Hubbard W. B., 2007, ApJ, 661, 502

Castelli F., Gratton R. G., Kurucz R. L., 1997, A&A, 318, 841

Charbonneau D., Brown T. M., Latham D. W., Mayor M., 2000, ApJL, 529, L45

Charbonneau D., Brown T. M., Noyes R. W., Gilliland R. L., 2002, ApJ, 568, 377

Collier Cameron A., Wilson D. M., West R. G., Hebb L., Wang X., Aigrain S., Bouchy F., Christian D. J., Clarkson W. I., Enoch B., Esposito M., Guenther E., Haswell C. A., Hébrard G., et al 2007, MNRAS, 380, 1230

Dunham E. W., Borucki W. J., Koch D. G., Batalha N. M., Buchhave L. A., Brown T. M., Caldwell D. A., Cochran W. D., Endl M., Fischer D., Fűrész G., Gautier T. N., Geary J. C., Gilliland R. L., et al 2010, ApJL, 713, L136

Enoch B., Cameron A. C., Parley N. R., Hebb L. H., 2010, An Improved Method for Estimating the Masses of Stars with Transiting Planets., arXiv:astro-ph/1004.1991v1

Fressin F., Guillot T., Morello V., Pont F., 2007, A&A, 475, 729

Gillon M., Anderson D. R., Triaud A. H. M. J., Hellier C., Maxted P. F. L., Pollacco D., Queloz D., 2009, A&A, 501, 785

Girardi L., Bressan A., Bertelli G., Chiosi C., 2000, VizieR Online Data Catalog, 414, 10371

Guillot T., Santos N. C., Pont F., Iro N., Melo C., Ribas I., 2006, A&A, 453, L21

Guillot T., Showman A. P., 2002, A&A, 385, 156

Hellier C., Anderson D. R., Gillon M., Lister T. A., Maxted P. F. L., Queloz D., Smalley B., Triaud A. H. M. J., West R. G., Wilson D. M., Alsubai K., Bentley S. J., Cameron A. C., Hebb L., Horne K., Irwin J., et al 2009, ApJL, 690, L89

Jackson B., Greenberg R., Barnes R., 2008, ApJ, 681, 1631

Jenkins J. M., Borucki W. J., Koch D. G., Marcy G. W., Cochran W. D., Basri G., Batalha N. M., Buchhave L. A., Brown T. M., Caldwell D. A., Dunham E. W., Endl M., Fischer D. A., Gautier III T. N., et al 2010, ArXiv e-prints

Konacki M., Torres G., Sasselov D. D., Jha S., 2005, ApJ, 624, 372

Kovács G., Bakos J. Á., Torres G., Sozzetti A., Latham D. W., Noyes R. W., Butler R. P., Marcy G. W., Fischer D. A., Fernández J. M., Esquerdo G., Sasselov D. D., Stefanik R. P., Pál A., Lázár J., Papp I., Sári P., 2007, ApJL, 670, L41

Latham D. W., Borucki W. J., Koch D. G., Brown T. M., Buchhave L. A., Basri G., Batalha N. M., Caldwell D. A., Cochran W. D., Dunham E. W., Fűrész G., Gautier T. N., Geary J. C., Gilliland R. L., et al 2010, ApJL, 713, L140

Laughlin G., Marcy G. W., Vogt S. S., Fischer D. A., Butler R. P., 2005, ApJL, 629, L121

Maxted P. F. L., Anderson D. R., Gillon M., Hellier C., Queloz D., Smalley B., Triaud A. H. M. J., West R. G., Wilson D. M., Bentley S. J., Collier Cameron A., Enoch B., Hebb L., Horne K.,

- Irwin J., et al 2010, ArXiv e-prints
- Mayor M., Udry S., Lovis C., Pepe F., Queloz D., Benz W., Bertaux J., Bouchy F., Mordasini C., Segransan D., 2009, A&A, 493, 639
- McCullough P. R., Stys J. E., Valenti J. A., Johns-Krull C. M., Janes K. A., Heasley J. N., Bye B. A., Dodd C., Fleming S. W., Pinnick A., Bissinger R., Gary B. L., Howell P. J., Vannmunder T., 2006, ApJ, 648, 1228
- Pollacco D., Skillen I., Collier Cameron A., Loeillet B., Stempels H. C., Bouchy F., Gibson N. P., Hebb L., Hébrard G., Joshi Y. C., McDonald I., Smalley B., Smith A. M. S., Street R. A., et al 2008, MNRAS, 385, 1576
- Pollacco D. L., Skillen I., Cameron A. C., Christian D. J., Hellier C., Irwin J., Lister T. A., Street R. A., West R. G., Anderson D., Clarkson W. I., Deeg H., Enoch B., Evans A., Fitzsimmons A., et al 2006, PASP, 118, 1407
- Pont F., Bouchy F., Queloz D., Santos N. C., Melo C., Mayor M., Udry S., 2004, A&A, 426, L15
- Rauer H., Queloz D., Csizmadia S., Deleuil M., Alonso R., Aigrain S., Almenara J. M., Auvergne M., Baglin A., Barge P., Bordé P., Bouchy F., Bruntt H., Cabrera J., Carone L., Carpano S., et al 2009, A&A, 506, 281
- Skillen I., Pollacco D., Collier Cameron A., Hebb L., Simpson E., Bouchy F., Christian D. J., Gibson N. P., Hébrard G., Joshi Y. C., Loeillet B., Smalley B., Stempels H. C., Street R. A., et al 2009, A&A, 502, 391
- Smalley B., Smith K., Dworetsky M., 2001,
<http://www.astro.keele.ac.uk/bs/publs/uclsyn.pdf>
- Stetson P. B., 1987, PASP, 99, 191
- Torres G., Andersen J., Giménez A., 2009, A&Arev, pp 13–+
- Torres G., Bakos J. Á., Kovács G., Latham D. W., Fernández J. M., Noyes R. W., Esquerdo G. A., Sozzetti A., Fischer D. A., Butler R. P., Marcy G. W., Stefanik R. P., Sasselov D. D., Lázár J., Papp I., Sári P., 2007, ApJL, 666, L121
- Triaud A., et al 2010, submitted, Preprint
- West R. G., Anderson D. R., Gillon M., Hebb L., Hellier C., Maxted P. F. L., Queloz D., Smalley B., Triaud A. H. M. J., Wilson D. M., Bentley S. J., Collier Cameron A., Enoch B., Horne K., Irwin J., Lister T. A., et al. 2009, AJ, 137, 4834
- West R. G., Collier Cameron A., Hebb L., Joshi Y. C., Pollacco D., Simpson E., Skillen I., Stempels H. C., Wheatley P. J., Wilson D., Anderson D., Bentley S., Bouchy F., Christian D., Enoch B., Gibson N., et al 2009, A&A, 502, 395